Enhanced expression of C/EBP homologous protein (CHOP) precedes degeneration of fibrocytes in the lateral wall after acute cochlear mitochondrial dysfunction induced by 3-nitropropionic acid

Yoshiaki Fujinami [a], Hideki Mutai [a], Kazusaku Kamiya [a], Kunio Mizutari [a], Masato Fujii [b], Tatsuo Matsunaga [a,*]

[a] Laboratory of Auditory Disorders, National Institute of Sensory Organs, National Tokyo Medical Center, 2-5-1 Higashigaoka, Meguro-ku, Tokyo 152-8902, Japan
[b] Division of Hearing and Balance Research, National Institute of Sensory Organs, National Tokyo Medical Center, Meguro-ku, Tokyo 152-8902, Japan

ARTICLE INFO

ABSTRACT

We previously reported that treatment of the rat cochlea with a mitochondrial toxin, 3-nitropropionic acid (3-NP), causes temporary to permanent hearing loss depending on the amount of the drug. Furthermore, apoptosis of cochlear lateral wall fibrocytes, which are important for maintaining the endolymph, is a predominant pathological feature in this animal model. 3-NP is known to induce oxidative stress as well as neuronal apoptosis. C/EBP homologous protein gene (*chop*) is one of the marker genes induced during endoplasmic reticulum (ER) stress, and is also considered to be involved in apoptosis. To elucidate the molecular mechanism of cochlear fibrocyte apoptosis induced by 3-NP, we studied spatiotemporal expression of C/EBP homologous protein (CHOP) and other signaling molecules related to ER stress as well as the appearance of apoptotic cells in the cochlear lateral wall after 3-NP treatment. Quantitative real-time PCR revealed that *chop* and activating transcription factor 4 gene (*atf-4*) showed marked increase within 6 h, whereas expression of other ER stress-responsive genes such as *grp78* and *grp94* did not change. Immunohistochemistry showed that 3-NP treatment caused up-regulation of CHOP, especially in type II and type IV fibrocytes, followed by the appearance of terminal deoxynucleotidyl transferase mediated dUTP nick end-labeling (TUNEL)-positive apoptotic cells in the same confined area. Thus, apoptosis of lateral wall fibrocytes induced by 3-NP is likely to be mediated by induction of CHOP. These results contribute clarification of pathological mechanism of cochlear fibrocytes and may lead to development of novel therapeutic strategy for hearing loss.

© 2009 Elsevier Ltd. All rights reserved.

1. Introduction

Recent advances in auditory research have helped build strategies to cure hearing loss by sensory cell regeneration or prevention of sensory cell loss (Holley, 2005; Kelley, 2006). Most experimental animal models of auditory disorders indicate that noise-induced, hereditary, and drug-induced hearing loss is caused by degeneration of the sensory hair cells or spiral ganglion cells. Recently, several studies reported the involvement of fibrocytes degeneration in the cochlear lateral wall (LW) in hereditary hearing loss (Minowa et al., 1999; Delprat et al., 2005), age-related hearing loss (Spicer and Schulte, 2002), and noise-induced hearing loss (Wang et al., 2002), implying that these non-sensory cells also play important roles in hearing.

We recently established an animal model of acute hearing loss, which is primarily caused by degeneration of LW fibrocytes, using the mitochondrial toxin 3-nitropropionic acid (3-NP) (Hoya et al., 2004; Okamoto et al., 2005; Kamiya et al., 2007; Mizutari et al., 2008). In this model, only less than a 2-fold difference in 3-NP dose differentiates between temporary and irreversible hearing loss. Appearance of TUNEL positive cells (Kamiya et al., 2007; Mizutari et al., 2008), and blockade of fibrocyte degeneration by caspase inhibitor (Mizutari et al., 2008) indicate that degeneration of LW fibrocytes is mainly apoptosis in this model. LW fibrocytes are critical for maintaining the ion concentration of the endolymph by K^+ recycling from the perilymph (Schulte and Steel, 1994; Spicer and Schulte, 1998); and disturbance of the endolymphatic ion concentration leads to immediate hearing loss. Fibrocytes of the LW are divided into five cell types based on structural features, immunostaining patterns and general location (Schulte and Adams, 1989; Spicer and Schulte, 1996; Mutai et al., 2009). Type II and type IV fibrocytes contain numerous mitochondria, and endoplasmic

reticulum (ER) expresses various types of ion transporters, channels, and pumps, and have significant roles in maintenance of the endolymph. 3-NP is considered to elicit acute deafness by depleting energy in the cochlea, which primarily induces apoptosis of type II and type IV fibrocytes followed by perturbation of endolymph homeostasis. Understanding the molecular pathway of LW fibrocytes cell death is likely to provide insight for preventing auditory disorders caused by LW fibrocyte dysfunction.

3-NP administration alters gene expression in various tissues and induces apoptosis in neuronal cells (Behrens et al., 1995; Pang and Geddes, 1997; Sato et al., 1997). C/EBP homologous protein (CHOP) is a DNA binding protein targeted by activating transcription factor 4 (ATF-4). *chop* (encoding CHOP) is one of the marker genes induced in ER stress (Oyadomari and Mori, 2004), which was originally defined as a cellular response against accumulation of unfolded proteins in the ER (Xu et al., 2005). In addition, the accumulation of unfolded proteins in mitochondria also induces CHOP expression (Zhao et al., 2002). CHOP is considered to be involved in apoptosis in various cell types (Matsumoto et al., 1996; Maytin et al., 2001). Part of the downstream pathways of CHOP that leads to apoptosis was recently revealed. It was reported that overexpression of Bcl-2 blocks CHOP-induced apoptosis (Matsumoto et al., 1996), Tribbles-related protein 3 (TRB3) repress the transcriptional activity of CHOP (Ohoka et al., 2005) and Bcl-2 interacting mediator of cell death (Bim) is closely related to the CHOP-induced apoptosis (Puthalakath et al., 2007). CHOP expression is induced in Parkinson's disease (Holtz and O'Malley, 2003), ischemia–reperfusion injury (Tajiri et al., 2004), and diabetes (Araki et al., 2003). The linkage between CHOP induction and cell death raises the possibility that CHOP may also play a role in eliciting apoptosis of LW fibrocytes exposed to 3-NP. To explore this possibility, we examined the induction of CHOP and other ER stress-related molecules such as *atf-4* gene (encoding an ATF-4) in the LW of 3-NP-treated animals, and the relationship of CHOP expression and apoptosis in the degenerating cells.

2. Results

2.1. Time course of hearing after 3-NP treatment

The time course of hearing in rats treated with 3-NP was measured by auditory brainstem response (ABR). Because our previous studies using the same animal model as the present study showed a remarkable difference in the time course of ABR thresholds at 8 kHz and 20 kHz between TTS and PTS rats, we measured ABR thresholds at these two frequencies in the present study. The rats treated with 300 mM 3-NP demonstrated severe hearing loss at both 8 kHz and 20 kHz (72.0 ± 5.9 dB and 85.5 ± 1.5 dB, respectively) 1 day after the treatment (DAT, Fig. 1). At 7 DAT, the threshold shift at 8 kHz recovered to almost the normal range (15.0 ± 1.2 dB) and the threshold shift at 20 kHz gradually recovered to a moderate level of hearing loss (40.0 ± 8.9 dB). These rats were referred as temporary threshold shift (TTS) rats. In contrast, the ABR threshold in rats treated with 500 mM 3-NP exceeded the highest measurable level at both tested frequencies 3 h after the treatment and did not show any signs of recovery even at 7 DAT. These rats were referred as permanent threshold shift (PTS) rats. Saline-treated rats maintained normal thresholds, indicating that the surgical procedures did not cause hearing loss. These phenotypes were consistent with our previous data (Hoya et al., 2004).

2.2. Time course of chop and atf-4 expression in the LW after 3-NP treatment

To explore the molecular events during hearing loss by 3-NP, we investigated whether the genes activated during ER stress were
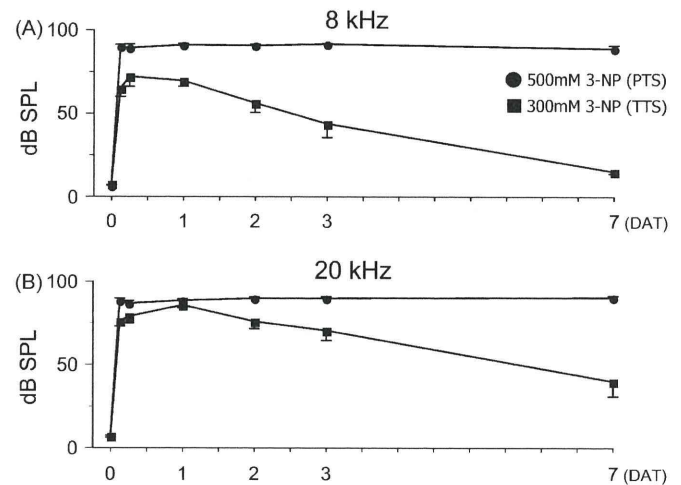

Fig. 1. Time course of auditory thresholds in temporary threshold shift (TTS) rats treated with 300 mM 3-nitropropionic acid (3-NP) and permanent threshold shift (PTS) rats treated with 500 mM 3-NP. The threshold shifts were recorded at 8 kHz (A) and 20 kHz (B). Although the thresholds reached their peak at 1 day after 3-NP treatment (DAT) and then decreased in the TTS rats, the thresholds in the PTS rats exceeded the measurable levels at 3 h after the treatment and were stable at 7 DAT. $n = 5$.

up-regulated in the LW after 3-NP treatment. Expression of four ER stress-responsive genes (*chop*, *atf-4*, *grp78*, and *grp94*) along with the housekeeping gene glyceraldehyde-3-phosphate dehydrogenase (*gapdh*) in the cochlear middle turn of TTS and PTS rats was measured using semi-quantitative reverse transcription PCR (RT-PCR). LW of cochlear middle turn was chosen because histological changes indicating degeneration of LW fibrocytes were evidently detected at this region in both TTS and PTS rats and there was a remarkable difference in the time course of ABR thresholds at this region between TTS and PTS rats.

We found that all five transcripts were successfully amplified in the LW from untreated rats (Fig. 2A). In addition, two of them, *chop* and its activator *atf-4*, both of which are suggested to be involved in activation of the apoptotic pathway, were up-regulated after 3-NP treatment. The changes in *chop* and *atf-4* expression from 3 h to 7 DAT were similar in the TTS and PTS rats; an increase of the PCR bands occurred in TTS and PTS rats within a few hours after treatment, but these band intensities dropped to the untreated levels in TTS rats and even lower in PTS rats at 1 DAT. In contrast, expression of *grp78* and *grp94*, molecular chaperones in the ER lumen and indicators of cell survival (Kaufman, 1999), did not show apparent changes throughout the experimental period (Fig. 2A), indicating that not all the genes mediating ER stress are stimulated in the LW after 3-NP treatment.

In the next experiment, expression levels of *chop* and *atf-4* after 3-NP treatment from which the changes were seen in the RT-PCR results were further evaluated by quantitative real-time RT-PCR (qPCR). These gene expressions were compared with those in untreated rats (0 DAT, $n = 5$). Because neither *grp78* nor *grp94* expression did not change in the screening by RT-PCR, these gene expressions were not measured by qPCR. The level of *chop* (Fig. 2B) was increased at 6 h after the treatment ($390 \pm 91\%$ in TTS rats, $p < 0.05$, and $595 \pm 262\%$ in PTS rats), confirming our previous observation that *chop* is induced promptly after 3-NP treatment. However, no significant difference in the peak level of *chop* was observed between PTS and TTS rats. At 1 DAT, the *chop* level dropped sharply to $53 \pm 6\%$ in TTS rats and $58 \pm 16\%$ in PTS rats, followed by gradual recovery to the untreated level in TTS and PTS rats until 7 DAT. As observed for *chop*, *atf-4* expression significantly increased and reached its peak 6 h after 3-NP treatment (Fig. 2C). The increase in *atf-4* expression was lower than that in *chop* both in TTS rats

(A)
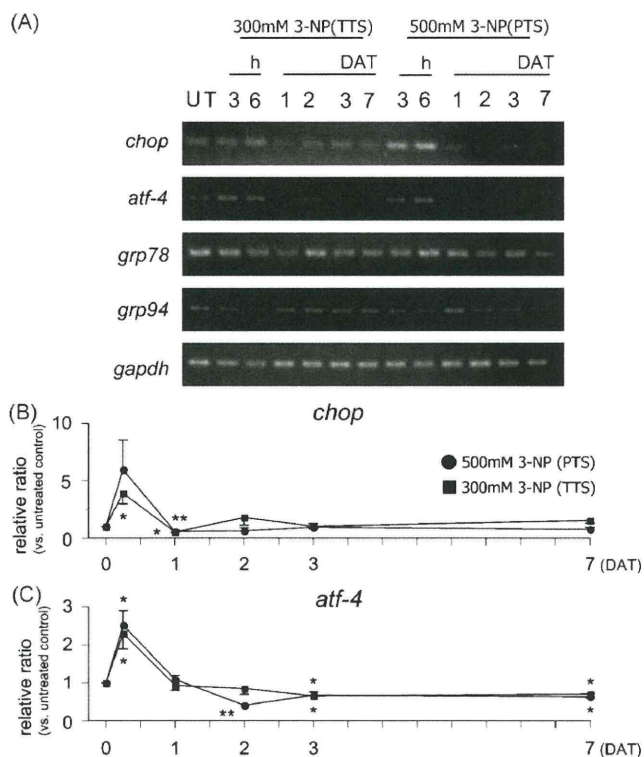
Fig. 2. Expression of ER stress-responsive genes in the lateral wall (LW) after 3-NP treatment. Expression was determined by semi-quantitative reverse transcription PCR (A) and quantitative real-time PCR (B and C). UT; untreated control rats; *gapdh*; glyceraldehyde-3-phosphate dehydrogenase. DAT; day(s) after 3-NP treatment. *chop* (B) and *atf-4* (C) were temporarily induced in the LW 6 h after treatment in both TTS rats treated with 300 mM 3-NP and PTS rats treated with 500 mM 3-NP. *chop* was decreased to approximately half of the untreated level (0 h) at 1 DAT and then recovered to the normal level. $n = 5$. $*p < 0.05$, $**p < 0.01$, significant difference vs. untreated control.

($230 \pm 40\%$, $p < 0.05$) and in PTS rats ($252 \pm 38\%$, $p < 0.05$). In the TTS and PTS rats, *atf-4* was down-regulated to $71 \pm 10\%$ and $64 \pm 8\%$ of the untreated level, respectively, at 7 DAT. Taken together, *chop* and *atf-4*, which are activated by various stimuli including ER stress, were responsive to 3-NP in the present study, whereas expression of the other candidate genes, *grp78* and *grp94*, did not change in response to the treatment.

2.3. Spatial expression patterns of CHOP and apoptosis in the LW after 3-NP treatment

We next investigated spatial expression patterns of the CHOP in the LW after 3-NP treatment. CHOP signals were detected using immunohistochemistry with paraformaldehyde-fixed, paraffin-embedded tissues. We focused on the cochlear middle turn to compare with expression levels of *chop* and *atf-4* by RT-PCR and qPCR. The same primary antibody for CHOP was used in this study as that used for a previous report (Hayashi et al., 2005). To ascertain specific binding of the primary antibody, a set of sections was stained in a similar way without the primary antibody, and the staining was not detected (data not shown). Types of LW fibrocytes were judged based on their localization within the spiral ligament according to the previous studies (Schulte and Adams, 1989; Spicer and Schulte, 1996; Mutai et al., 2009). Fig. 3 shows distribution of the CHOP signal at the middle turn of the LW before and after 3-NP treatment. CHOP was detected at low levels in the LW of untreated and saline-treated rats (Fig. 3A and F). The low CHOP signal level persisted until 6 h after treatment in both TTS and PTS rats (Fig. 3B and G). The CHOP signal intensity started to increase over the entire spiral ligament at 1 DAT in both TTS and PTS rats (Fig. 3C and

H), with the most intense staining in the area of type II and type IV fibrocytes in PTS rats. At this time in the TTS, CHOP immunoreactivity was localized mainly in the cytoplasm (Fig. 3C and L), and localized slightly also in the nuclei. CHOP immunoreactivity did not remain in the LW at 2 DAT (Fig. 3D). On the other hand, immunoreactivity in the PTS rats at 1 DAT was localized mainly in the nuclei (Fig. 3H and N), and remained in the LW at 2DAT and 3 DAT (Fig. 3I and J). Fibrocyte degeneration was not apparent in the spiral ligament of either TTS or PTS rats until 1 DAT. In TTS rats, fibrocyte degeneration which was indicated by a region free of cellular nuclei was observed in the area of type II and type IV fibrocytes at 2 DAT (Fig. 3D and M) and 3 DAT (Fig. 3E) and area of fibrocyte degeneration did not expand from 2 DAT to 3 DAT. In PTS rats, a subpopulation of type II and type IV fibrocytes started to disappear and CHOP immunoreactivity was detected around this area at 2 DAT (Fig. 3I and O), and a majority of the fibrocytes in the LW had degenerated at 3 DAT (Fig. 3J).

Because our previous study showed that death of LW fibrocytes is mediated by an apoptotic pathway (Kamiya et al., 2007; Mizutari et al., 2008), we next investigated whether the onset of apoptotic cell death coincides with the onset of CHOP induction. The paraffin sections were used for the terminal deoxynucleotidyl transferase mediated dUTP nick end-labeling (TUNEL) assay, a method generally accepted to detect DNA fragmentation caused by activation of apoptotic pathways (Fig. 4). TUNEL-positive cells were not detected in untreated and saline-treated LWs (Fig. 4A and F). In TTS rats (Fig. 4B–E), TUNEL-positive cells appeared at 2 DAT in the area of type II fibrocytes (Fig. 4D and M). A small number of TUNEL-positive cells were also evident at 3 DAT (Fig. 4E). In PTS rats (Fig. 4G–J), TUNEL-positive cells were detectable as early as 1 DAT in the type II/IV fibrocytes (Fig. 4H). The number of TUNEL-positive cells in the LW gradually increased from 1 to 3 DAT (Fig. 4H–J). To clarify whether CHOP induction and apoptotic cell death are associated, the LWs in the untreated or PTS rats were subjected to a double immunofluorescence study (Fig. 5A–J). CHOP signal (red) was low in untreated rats (Fig. 5A, D, E) and intensified in the area of type II and type IV fibrocytes at 1 DAT in PTS rats (Fig. 5F, I, and J). TUNEL-positive apoptotic cells (green) were undetectable in the LW of untreated rats (Fig. 5B, D, and E) but were observed in PTS rats at 1 DAT (Fig. 5G, I, and J). Although apoptotic cells were not convincingly co-immunostained with CHOP in PTS rats at 1 DAT, they were confined to the CHOP-positive area (Fig. 5I and J). In untreated rats, the CHOP signal visualized by fluorescein staining in the stria vascularis (Fig. 5A) was inconsistent with the absence of a signal in the stria vascularis by 3,3′-diaminobenzidine (DAB) staining (Fig. 3A). The difference was considered to be due to the methods used for antigen retrieval. Because apoptotic cells were not detected in the stria vascularis, we focused on the CHOP expression in the spiral ligament. Thus, CHOP expression in the stria vascularis is not discussed further in this study. Overall, we demonstrated that induction of the CHOP signal was followed by apoptotic cell death in the LW fibrocytes after 3-NP treatment.

3. Discussion

In this study, we examined the time course of CHOP expression, apoptosis, and degeneration of fibrocytes after administration of 3-NP. We demonstrated temporary CHOP expression in the confined area of LW in which fibrocyte degeneration occurred afterwards. In TTS rats, TUNEL-positive cells became detectable at 2 DAT, approximately 1 day after CHOP induction. In PTS rats, a few TUNEL-positive cells were detectable at 1 DAT, when the CHOP level was first up-regulated. Then, the number of TUNEL-positive cells increased significantly at 2 DAT. CHOP and TUNEL signals are detectable in the same area, but co-localization of these two
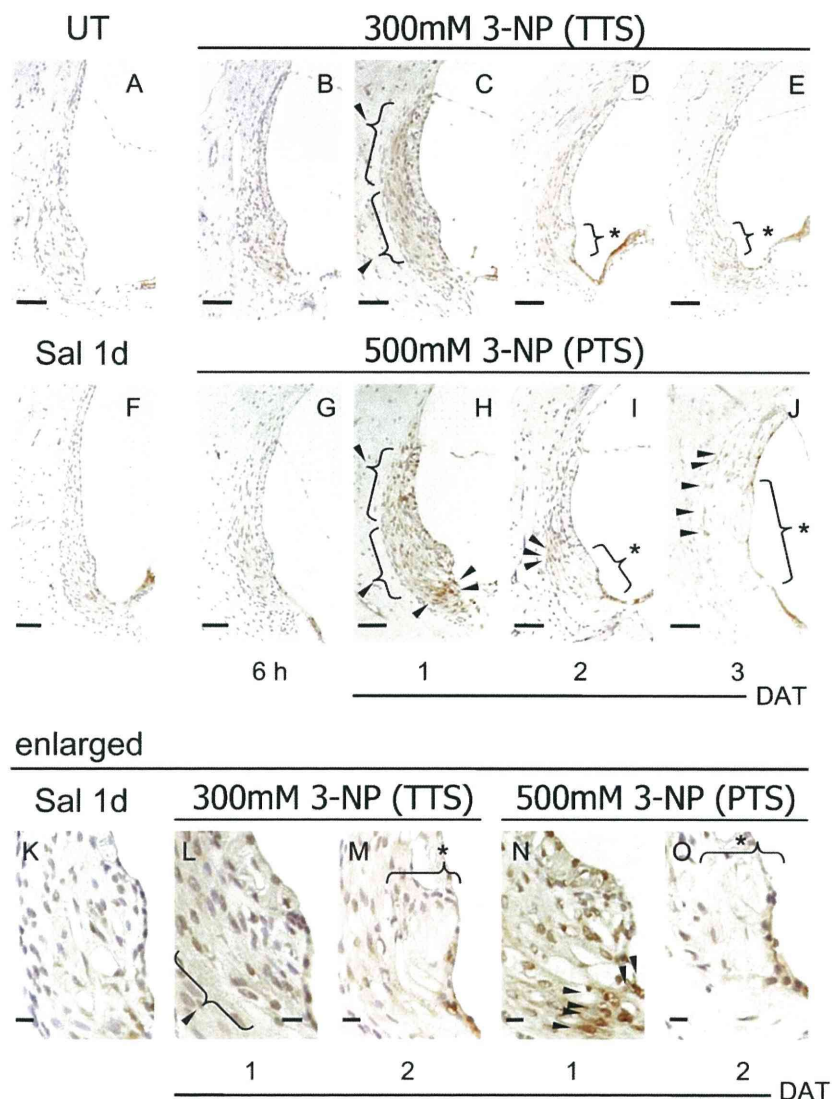
Fig. 3. Immunohistochemical analysis of CHOP expression in the LW after 3-NP treatment. In untreated control rats (UT), a low level of CHOP was detectable in the entire LW (A). In TTS rats treated with 300 mM 3-NP (B–E, L, and M), the CHOP signal (arrowheads) was unchanged at 6 h but intensified 1 day after 3-NP treatment (DAT) (C) compared with saline-treated rats (Sal 1d, F, K). A limited area (asterisk) of the LW had degenerated at 2 DAT and 3 DAT (D, E). In PTS rats treated with 500 mM 3-NP (G–J, N, and O), an intense CHOP signal (arrowheads) was evident, especially in the area of type II and type IV fibrocytes of the LW at 1 DAT (H). At 2 DAT, type II and type IV fibrocytes appeared to start degeneration (asterisk) (I), and the area of degenerated fibrocytes expanded at 3 DAT (J). K–O are enlarged images of spiral prominence of F, C, D, H and I, respectively. Scale bar = 50 μm (A–J) and 10 μm (K–O).

staining was not detected. Because CHOP is known to be involved in inducing apoptosis (Matsumoto et al., 1996; Maytin et al., 2001), we speculate that the delay of TUNEL appearance is due to signal transduction for apoptotic pathways. Tajiri et al. (2004) reported that *chop* induction in the striatum peaks 12 h after the occlusion of the carotid artery, followed by detection of numerous TUNEL-positive cells at 24 h. Investigation of signaling molecules downstream of CHOP (Wang et al., 1998; Sok et al., 1999) and activation of pro-apoptotic molecules such as caspases after 3-NP treatment may clarify the direct association of CHOP activation with apoptotic cell death in LW fibrocytes. In the present study, of note is that nuclei were also positively stained for CHOP in PTS rats at 1 DAT, which is required to exert functional effect for this transcription factor (Zinszner et al., 1998).

The activation of ATF-4 and CHOP in the LW of 3-NP-treated rats is reminiscent of CHOP and ATF-4 activation in ischemic brain (Hayashi et al., 2005). Induction of the same molecules in these two affected areas is probably caused by the features of energy depletion which are shared by mitochondrial dysfunction and ischemia. What is the mechanism of the expression of *atf-4* and

CHOP which is the downstream target of ATF-4 in LW fibrocytes? The mitochondrial toxin 3-NP is an irreversible inhibitor of succinate dehydrogenase (complex II of the electron transport chain) (Coles et al., 1979). Inhibition of energy metabolism by 3-NP results in the production of reactive oxygen species (Beal et al., 1995; Lee et al., 2002; Rosenstock et al., 2004) that causes oxidative stress and neuronal cell death (Behrens et al., 1995; Pang and Geddes, 1997; Sato et al., 1997; Higuchi, 2004). Oxidative stress induces ER stress (Yu et al., 1999), and this is known to enhance CHOP expression (Oyadomari and Mori, 2004). In addition, cells exposed to 3-NP also release mitochondrial Ca^{2+}, which is caused by an increasing amount of reactive oxygen species (Rosenstock et al., 2004) and rapid elevation of the intracellular Ca^{2+} level is known to enhance CHOP expression (Deshpande et al., 1997; Tanaka et al., 2005). Thus, oxidative stress, ER stress and increase in the intracellular Ca^{2+} level are related events in terms of the molecular signaling pathways. We assume 3-NP induced ATF-4 and CHOP in LW by these mechanism.

Our findings are not in full agreement with the hypothesis that CHOP is activated exclusively in response to ER stress in the LW
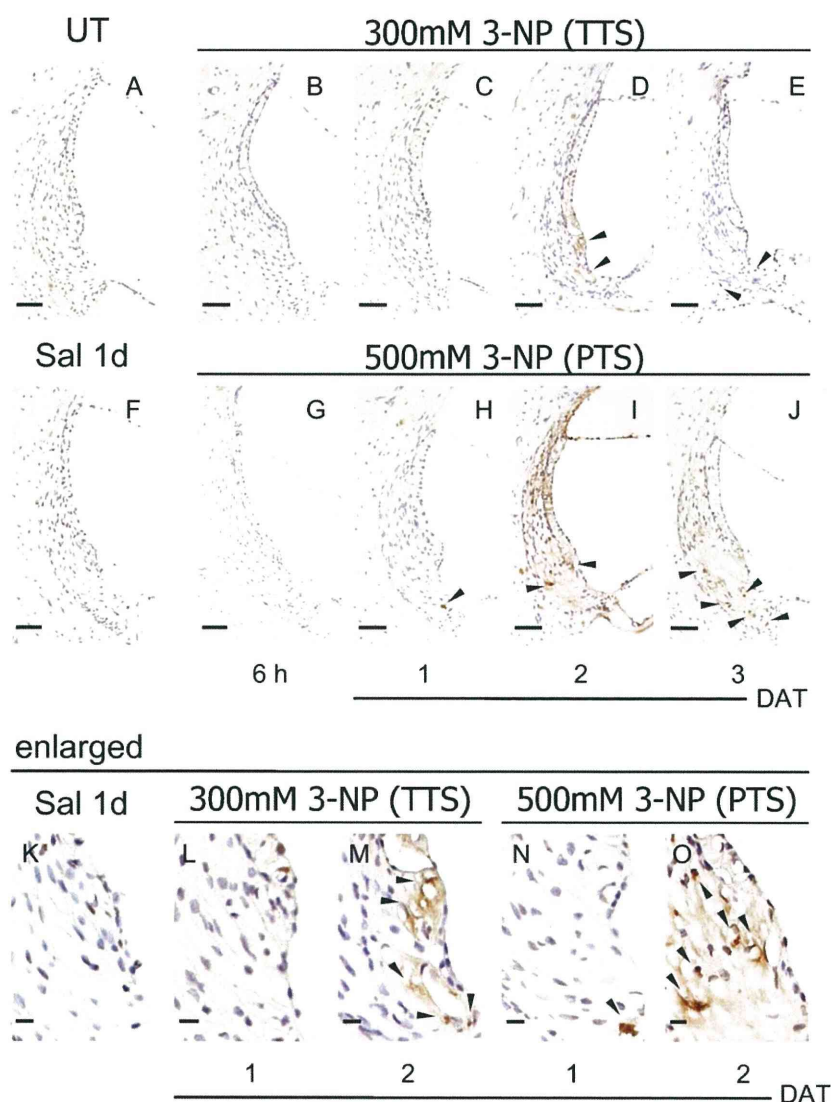
Fig. 4. TUNEL histochemical analysis of apoptotic cells in the LW after 3-NP treatment. Apoptotic cells were not detected in untreated control rats (UT; A) or in saline-treated rats (Sal 1d; F). In TTS rats treated with 300 mM 3-NP (B–E), a small number of apoptotic cells (arrowheads) were found at 2 DAT and 3 DAT (D, E). In PTS rats treated with 500 mM 3-NP (G–J), apoptotic cells were detectable at 1 DAT (H). The number of apoptotic cells (arrowheads) increased as the degenerating area expanded at 2 DAT and 3 DAT (I, J). K–O are enlarged images of spiral prominence of F, C, D, H and I, respectively. Scale bar = 50 μm (A–J) and 10 μm (K–O).

treated with 3-NP, because multiple attempts failed to show significant up-regulation of the ER stress mediators *grp78* and *grp94*. These results suggest that either a partial ER stress-response pathway including ATF-4 and CHOP is activated, or that mechanisms other than ER stress are responsible for the activation of the two molecules in the LW treated with 3-NP. CHOP has been reported to be induced without activation of other ER stress-responsive proteins such as GRP78 in a cultural experimental model of mitochondrial stress (Zhao et al., 2002). In this model, accumulation of unfolded proteins in the mitochondria resulted in induction of CHOP and mitochondrial molecular chaperones (e.g., Cpn60, Cpn10 and mtDnaJ), but did not induce non-mitochondrial chaperones including GRP78. Moisoi et al. (2009) also reported that *chop* expression was increased by mitochondrial dysfunction in the brain. Similarly, induction of *atf-4* and *chop* in the LW after 3-NP treatment may also be caused by mitochondrial stress following oxidative stress. On the other hand, investigation of PERK, IRE-1 and ATF-6 is necessary to demonstrate that ER stress is concerned with the increase of *chop* expression in this study.

The expression levels of *chop* at 6 h after 3-NP treatment and at 1 DAT were not significantly different between TTS and PTS rats,

despite the contrasting number of degenerating cells at 3 DAT. Immunohistochemical study revealed nuclear staining of CHOP, which is required to undergo functional role for transcription factor, in PTS rats but rarely in TTS rats. This may explain the different levels of apoptosis at 3 DAT. Another possibility is that CHOP may be involved in the only initial induction of apoptosis in this model and another death pathway which sustained ongoing cell death was also activated in PTS rats but not activated in TTS rats. Further study to identify regulators of degeneration in LW fibrocytes will provide us with insight to develop strategies to prevent death of LW fibrocytes.

In summary, we characterized a novel molecular mechanism of acute hearing loss caused by 3-NP administration and identified CHOP, a mediator of oxidative stress, ER stress, and mitochondrial stress, as a preceding marker of damage in LW fibrocytes.

4. Experimental procedures

4.1. Animals and drug administration

Male Sprague–Dawley rats (6–8 weeks old, weighing 170–230 g) were used. The rats were housed in metallic breeding cages in a room with a light/dark
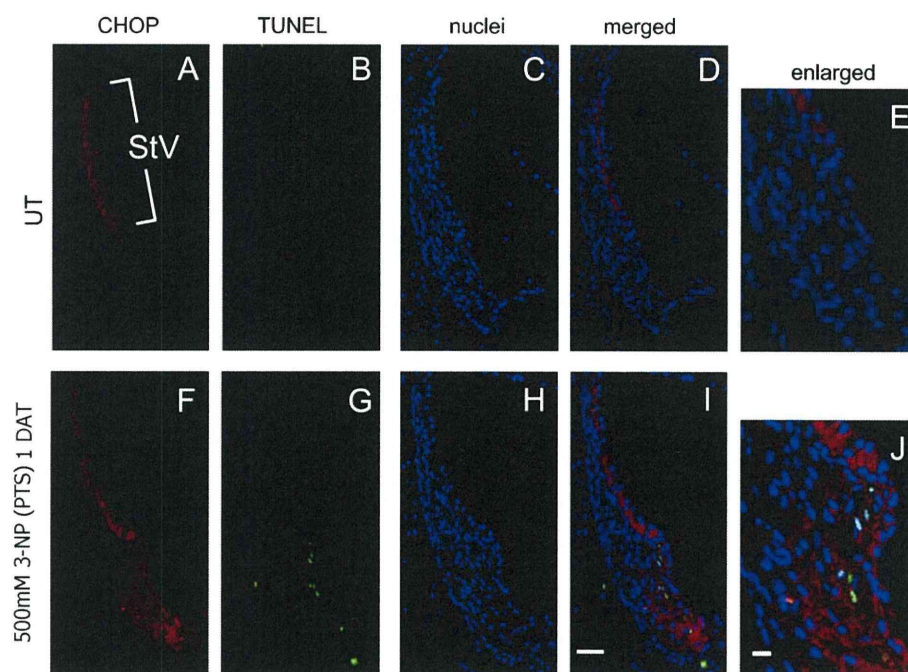
Fig. 5. Concurrent detection of CHOP and apoptosis in the LW after 3-NP treatment. The LW of untreated control rats (UT; A–E) and PTS rats treated with 500 mM 3-NP (F–J) were double-immunostained with antibodies to CHOP (red) and TUNEL (green), and counterstained with DAPI for nuclear staining (blue). Although apoptotic cells were not observed in untreated rats (B, D, and E), apoptosis was detected in the area of type II and type IV fibrocytes in PTS rats 1 day after 3-NP treatment (PTS rats 1 DAT; G) where the CHOP signal was enhanced (F, I, J). E and J were enlarged images of spiral prominence of D and H, respectively. StV; stria vascularis. Scale bar = 50 μm (A–D, F–I) and 10 μm (E, J). (For interpretation of the references to color in this figure legend, the reader is referred to the web version of the article.)

Table 1
PCR primers and their target genes used in the study.

Gene	Acc. number	Sequence (5′ > 3′)		Product length (bp)	Annealing temperature (°C)
		Forward	Reverse		
chop	U30186	AGTCTCTGCCTTTCGCCTTT	GCCACTTTCCTCTCATTCTC	382	55.4
atf-4	NM_024403	GCTGCCCCCTTTACATTCTT	AGCACAAAGCACCTGACTAC	615	54.5
grp78	XM_213908	AACGACCCCTGACAAAAGAC	TAGCCAATTCCTCCTCTCCC	768	57.9
grp94	XM_343192	ACACGGCTTGCTAAACTTCT	CTCTGGCTCTTCCTCTACCT	771	54.2
gapdh	M17701	GCCAAAAGGGTCATCATCTC	GCCTCTCTCTTGCTCTCAGT	715	55.5

Abbreviations: Acc. number: accession number; *chop*: C/EBP homologous protein; *atf-4*: activating transcription factor-4; *grp78* and *grp94*: glucose-regulated protein 78 and 94; *gapdh*: glyceraldehyde-3-phosphate dehydrogenase.

cycle of 12 h and humidity of 55% at 23 °C, with free access to food and water for at least 7 days before use. In these rats, hearing loss was induced by surgical administration of different concentrations of 3-NP onto the inner ear (Hoya et al., 2004). Before surgery, the rats were anesthetized with pentobarbital (40–50 mg/kg, i.p.) or pentobarbital (20–25 mg/kg, i.p.), ketamine (40–60 mg/kg, i.p.) and xylazine (4–6 mg/kg, i.p.). An incision was made posterior to the left pinna near the external meatus after local administration of lidocaine (1%). The left otic bulla was opened to approach the round window niche. The tip of a polyethylene tube (PE10, Becton Dickinson & Co., Franklin Lakes, NJ) was drawn to a fine tip in a flame and gently inserted into the round window niche. 3-NP (Sigma, St. Louis, MO) was dissolved in saline at 300 mM or 500 mM and the pH was adjusted to 7.4 with NaOH. Each 3-NP solution (3 μL) was administered with a syringe pump. Following 3-NP treatment, a tiny piece of gelatin was placed on the niche to keep the solution in the niche during head movement after awakening from anesthesia, and the wound was closed (Hoya et al., 2004; Okamoto et al., 2005). All the experimental procedures were performed in accordance with guidelines from the National Tokyo Medical Center, and were approved by the Animal Care and Use Committee of the Institute. Adequate measures were taken to minimize pain or discomfort of experimental animals.

4.2. Measurement of auditory brainstem response

ABRs were recorded from each rat before 3-NP treatment, and 3 h, 6 h, 1, 2, 3 and 7 days after 3-NP treatment. Pure tone bursts of 8 kHz and 20 kHz (0.2 ms rise/fall time 1 ms flat segment) were used, and auditory thresholds in the treated ear were measured at the same time point using incremental steps of 5 dB. Details of ABR recording were previously described (Hoya et al., 2004).

4.3. Semi-quantitative reverse transcription PCR

After the rats were anesthetized from each rat before 3-NP treatment, and 3 h, 6 h, 1, 2, 3 and 7 days after 3-NP treatment (n = 5), temporal bones were quickly removed and immersed in RNA later (Takara Bio, Shiga, Japan) on ice, followed by dissection of the middle turn of the LW. Total RNA was isolated using TRIzol reagent (cultural gen, Carlsbad, CA) according to the manufacturer's protocol. Total RNA was extracted by DEPC-treated water and the purity of total RNA was measured with a UV/visible spectrophotometer (Ultrospec 2100 pro; Amersham Pharmacia Biotech, Piscataway, NJ) by the ratio of OD_{260}/OD_{280}. First-strand cDNA synthesis was performed using 100 ng of total RNA and oligo(dT)$_{12–18}$ primers in a total volume of 20 μL according to the SuperScript III RNase H⁻ Reverse Transcriptase protocol (cultural gen). We used PCR primers specific for *chop*, *atf-4*, glucose-regulated protein *grp78* and *grp94*, and *gapdh*. The sequences of the PCR primers, sizes of the predicted PCR products, and the annealing temperature are listed in Table 1. The target genes were amplified in 25 μL of reaction containing 2.5 μL of diluted cDNA, 0.2 μM of each dNTP, 0.4 μM of each primer, 0.625 U of Taq DNA polymerase (Sigma) and 1× buffer (10 mM Tris–HCl (pH 8.3), 50 mM KCl, 1.5 mM MgCl$_2$ and 0.001% gelatin). PCR was conducted at 94 °C for 5 min, 30 cycles of 94 °C for 1 min, the specific annealing temperature for 1 min, and 72 °C for 2 min, followed by 72 °C for 10 min, and then 10 μL of each PCR product was analyzed by 1% agarose gel electrophoresis in Tris–acetate-EDTA buffer. PCR products were electrophoresed and visualized using ethidium bromide. The images were captured by CS Analyzer (Atto, Tokyo, Japan).

4.4. Quantitative real-time RT-PCR analysis

qPCR was performed according to manufacturer's protocols for the ABI PRISM 7000 Sequence Detection System (Applied Biosystems, Foster City, CA). The

identical cDNAs prepared for RT-PCR were used as the templates for qPCR. Specific primer sets were purchased from Takara Bio. qPCR was performed in 25 μL of reaction mixture containing 1 × SYBR Premix Ex Taq (Takara Bio), 1 × ROX Reference Dye, 0.2 μM of each primer and cDNA. PCR was conducted for 5 s at 95 °C and 31 s at 60 °C for 40 cycles. Gene expression levels were normalized using *gapdh* as an internal control. Results of ABR and qPCR are expressed as the mean ± standard error, and statistical significance was determined by one sample *t*-test.

4.5. Immunohistochemical analysis

Histological sample were made on the before 3-NP treatment and 1 day after vehicle treatment, and 6 h, 1, 2 and 3 days after 3-NP treatment ($n \geq 3$). Rats were deeply anesthetized with pentobarbital (50 mg/kg, i.p.) and perfused intracardially with 0.01 M sodium phosphate buffer (pH 7.4) containing 8.6% sucrose, followed by 4% paraformaldehyde in 0.1 M sodium phosphate buffer (pH 7.4). After decapitation, temporal bones were removed quickly and placed in the same 4% paraformaldehyde fixative. Small openings were made at the round window, oval window and apex of the cochlea. After immersion in the fixative overnight, the temporal bones were decalcified by placement in 5% EDTA and 4% sucrose in 0.1 M sodium phosphate buffer (pH 7.4) at 4 °C for 2 weeks, dehydrated, and embedded in paraffin. Transverse cochlear sections at 5-μm thickness were cut and mounted on glass slides. After rehydration, sections were treated with 0.3% hydrogen peroxide in methanol to quench peroxidase activity. For epitope retrieval, slides were boiled in citrate buffer (pH 6.0) in a microwave. After blocking nonspecific binding with 1% normal goat serum (Vector Laboratories, Burlingame, CA), the slides were incubated with monoclonal anti-CHOP (Santa Cruz Biotechnology, Santa Cruz, CA) at a 1:100 dilution at 4 °C overnight. The slides were washed and then incubated with biotinylated anti-mouse IgG (Vector Laboratories) at a 1:200 dilution, and the signal was colorized using VECTASTAIN Elite ABC kit (Vector Laboratories) and DAB Substrate kit for Peroxidase (Vector Laboratories). Some of the slides were counterstained with hematoxylin. Some of the unstained sections were processed for TUNEL histochemical staining using ApopTag Peroxidase In Situ Apoptosis Detection kit (Chemicon International, Temecula, CA) according to the manufacturer's protocol. The TUNEL reaction mixture was added to each sample in a humidified chamber, followed by incubation for 1 h at 37 °C for colorization with DAB. For fluorescent immunostaining, the sections were incubated with anti-CHOP at a dilution of 1:50. The sections were subsequently treated with proteinase K (DakoCytomation, Carpinteria, CA) and incubated with Alexa Fluor 568 anti-mouse IgG (Molecular Probes, Eugene, OR) at a 1:1000 dilution. Thereafter, the ApopTag Fluorescein Direct In Situ Apoptosis Detection kit (Chemicon) was used according to the manufacturer's protocol. The sections were then covered with PermaFluor Aqueous Mounting Medium (Thermo Shandon, Pittsburgh, PA) with DAPI (1 μg/mL; Dojindo, Kumamoto, Japan).

Acknowledgements

References

Araki, E., Oyadomari, S., Mori, M., 2003. Impact of endoplasmic reticulum stress pathway on pancreatic beta-cells and diabetes mellitus. Exp. Biol. Med. (Maywood) 228, 1213–1217.

Beal, M.F., Ferrante, R.J., Henshaw, R., Matthews, R.T., Chan, P.H., Kowall, N.W., Epstein, C.J., Schulz, J.B., 1995. 3-Nitropropionic acid neurotoxicity is attenuated in copper/zinc superoxide dismutase transgenic mice. J. Neurochem. 65, 919–922.

Behrens, M.I., Koh, J., Canzoniero, L.M., Sensi, S.L., Csernansky, C.A., Choi, D.W., 1995. 3-Nitropropionic acid induces apoptosis in cultured striatal and cortical neurons. Neuroreport 6, 545–548.

Coles, C.J., Edmondson, D.E., Singer, T.P., 1979. Inactivation of succinate dehydrogenase by 3-nitropropionate. J. Biol. Chem. 254, 5161–5167.

Delprat, B., Ruel, J., Guitton, M.J., Hamard, G., Lenoir, M., Pujol, R., Puel, J.L., Brabet, P., Hamel, C.P., 2005. Deafness and cochlear fibrocyte alterations in mice deficient for the inner ear protein otospiralin. Mol. Cell. Biol. 25, 847–853.

Deshpande, S.B., Fukuda, A., Nishino, H., 1997. 3-Nitropropionic acid increases the intracellular Ca^{2+} in cultured astrocytes by reverse operation of the Na^{+}-Ca^{2+} exchanger. Exp. Neurol. 145, 38–45.

Hayashi, T., Saito, A., Okuno, S., Ferrand-Drake, M., Dodd, R.L., Chan, P.H., 2005. Damage to the endoplasmic reticulum and activation of apoptotic machinery by oxidative stress in ischemic neurons. J. Cereb. Blood Flow Metab. 25, 41–53.

Higuchi, Y., 2004. Glutathione depletion-induced chromosomal DNA fragmentation associated with apoptosis and necrosis. J. Cell. Mol. Med. 8, 455–464.

Holley, M.C., 2005. Keynote review: the auditory system, hearing loss and potential targets for drug development. Drug Discov. Today 10, 1269–1282.

Holtz, W.A., O'Malley, K.L., 2003. Parkinsonian mimetics induce aspects of unfolded protein response in death of dopaminergic neurons. J. Biol. Chem. 278, 19367–19377.

Hoya, N., Okamoto, Y., Kamiya, K., Fujii, M., Matsunaga, T., 2004. A novel animal model of acute cochlear mitochondrial dysfunction. Neuroreport 15, 1597–1600.

Kamiya, K., Fujinami, Y., Hoya, N., Okamoto, Y., Kouike, H., Komatsuzaki, R., Kusano, R., Nakagawa, S., Satoh, H., Fujii, M., Matsunaga, T., 2007. Mesenchymal stem cell transplantation accelerates hearing recovery through the repair of injured cochlear fibrocytes. Am. J. Pathol. 171, 214–226.

Kaufman, R.J., 1999. Stress signaling from the lumen of the endoplasmic reticulum: coordination of gene transcriptional and translational controls. Genes Dev. 13, 1211–1233.

Kelley, M.W., 2006. Regulation of cell fate in the sensory epithelia of the inner ear. Nat. Rev. Neurosci. 7, 837–849.

Lee, W.T., Yin, H.S., Shen, Y.Z., 2002. The mechanisms of neuronal death produced by mitochondrial toxin 3-nitropropionic acid: the roles of N-methyl-D-aspartate glutamate receptors and mitochondrial calcium overload. Neuroscience 112, 707–716.

Matsumoto, M., Minami, M., Takeda, K., Sakao, Y., Akira, S., 1996. Ectopic expression of CHOP (GADD153) induces apoptosis in M1 myeloblastic leukemia cells. FEBS Lett. 395, 143–147.

Maytin, E.V., Ubeda, M., Lin, J.C., Habener, J.F., 2001. Stress-inducible transcription factor CHOP/gadd153 induces apoptosis in mammalian cells via p38 kinase-dependent and -independent mechanisms. Exp. Cell Res. 267, 193–204.

Minowa, O., Ikeda, K., Sugitani, Y., Oshima, T., Nakai, S., Katori, Y., Suzuki, M., Furukawa, M., Kawase, T., Zheng, Y., Ogura, M., Asada, Y., Watanabe, K., Yamanaka, H., Gotoh, S., Nishi-Takeshima, M., Sugimoto, T., Kikuchi, T., Takasaka, T., Noda, T., 1999. Altered cochlear fibrocytes in a mouse model of DFN3 nonsyndromic deafness. Science 285, 1408–1411.

Mizutari, K., Matsunaga, T., Kamiya, K., Fujinami, Y., Fujii, M., Ogawa, K., 2008. Caspase inhibitor facilitates recovery of hearing by protecting the cochlear lateral wall from acute cochlear mitochondrial dysfunction. J. Neurosci. Res. 86, 215–222.

Moisoi, N., Klupsch, K., Fedele, V., East, P., Sharma, S., Renton, A., Plun-Favreau, H., Edwards, R.E., Teismann, P., Esposti, M.D., Morrison, A.D., Wood, N.W., Downward, J., Martins, L.M., 2009. Mitochondrial dysfunction triggered by loss of HtrA2 results in the activation of a brain-specific transcriptional stress response. Cell Death Differ. 16, 449–464.

Mutai, H., Nagashima, R., Fujii, M., Matsunaga, T., 2009. Mitotic activity and specification of fibrocyte subtypes in the developing rat cochlear lateral wall. Neuroscience 163, 1255–1263.

Ohoka, N., Yoshii, S., Hattori, T., Onozaki, K., Hayashi, H., 2005. TRB3, a novel ER stress-inducible gene, is induced via ATF4-CHOP pathway and is involved in cell death. Embo J. 24, 1243–1255.

Okamoto, Y., Hoya, N., Kamiya, K., Fujii, M., Ogawa, K., Matsunaga, T., 2005. Permanent threshold shift caused by acute cochlear mitochondrial dysfunction is primarily mediated by degeneration of the lateral wall of the cochlea. Audiol. Neurootol. 10, 220–233.

Oyadomari, S., Mori, M., 2004. Roles of CHOP/GADD153 in endoplasmic reticulum stress. Cell Death Differ. 11, 381–389.

Pang, Z., Geddes, J.W., 1997. Mechanisms of cell death induced by the mitochondrial toxin 3-nitropropionic acid: acute excitotoxic necrosis and delayed apoptosis. J. Neurosci. 17, 3064–3073.

Puthalakath, H., O'Reilly, L.A., Gunn, P., Lee, L., Kelly, P.N., Huntington, N.D., Hughes, P.D., Michalak, E.M., McKimm-Breschkin, J., Motoyama, N., Gotoh, T., Akira, S., Bouillet, P., Strasser, A., 2007. ER stress triggers apoptosis by activating BH3-only protein Bim. Cell 129, 1337–1349.

Rosenstock, T.R., Carvalho, A.C., Jurkiewicz, A., Frussa-Filho, R., Smaili, S.S., 2004. Mitochondrial calcium, oxidative stress and apoptosis in a neurodegenerative disease model induced by 3-nitropropionic acid. J. Neurochem. 88, 1220–1228.

Sato, S., Gobbel, G.T., Honkaniemi, J., Li, Y., Kondo, T., Murakami, K., Sato, M., Copin, J.C., Chan, P.H., 1997. Apoptosis in the striatum of rats following intraperitoneal injection of 3-nitropropionic acid. Brain Res. 745, 343–347.

Schulte, B.A., Adams, J.C., 1989. Distribution of immunoreactive Na+, K+-ATPase in gerbil cochlea. J. Histochem. Cytochem. 37, 127–134.

Schulte, B.A., Steel, K.P., 1994. Expression of alpha and beta subunit isoforms of Na, K-ATPase in the mouse inner ear and changes with mutations at the Wv or Sld loci. Hear. Res. 78, 65–76.

Sok, J., Wang, X.Z., Batchvarova, N., Kuroda, M., Harding, H., Ron, D., 1999. CHOP-dependent stress-inducible expression of a novel form of carbonic anhydrase VI. Mol. Cell. Biol. 19, 495–504.

Spicer, S.S., Schulte, B.A., 1996. The fine structure of spiral ligament cells relates to ion return to the stria and varies with place-frequency. Hear. Res. 100, 80–100.

Spicer, S.S., Schulte, B.A., 1998. Evidence for a medial K+ recycling pathway from inner hair cells. Hear. Res. 118, 1–12.

Spicer, S.S., Schulte, B.A., 2002. Spiral ligament pathology in quiet-aged gerbils. Hear. Res. 172, 172–185.

Tajiri, S., Oyadomari, S., Yano, S., Morioka, M., Gotoh, T., Hamada, J.I., Ushio, Y., Mori, M., 2004. Ischemia-induced neuronal cell death is mediated by the endoplasmic reticulum stress pathway involving CHOP. Cell Death Differ. 11, 403–415.

Tanaka, K., Tomisato, W., Hoshino, T., Ishihara, T., Namba, T., Aburaya, M., Katsu, T., Suzuki, K., Tsutsumi, S., Mizushima, T., 2005. Involvement of intracellular Ca^{2+} levels in nonsteroidal anti-inflammatory drug-induced apoptosis. J. Biol. Chem. 280, 31059–31067.

Wang, X.Z., Kuroda, M., Sok, J., Batchvarova, N., Kimmel, R., Chung, P., Zinszner, H., Ron, D., 1998. Identification of novel stress-induced genes downstream of chop. EMBO J. 17, 3619–3630.

Wang, Y., Hirose, K., Liberman, M.C., 2002. Dynamics of noise-induced cellular injury and repair in the mouse cochlea. J. Assoc. Res. Otolaryngol. 3, 248–268.

Xu, C., Bailly-Maitre, B., Reed, J.C., 2005. Endoplasmic reticulum stress: cell life and death decisions. J. Clin. Invest. 115, 2656–2664.

Yu, Z., Luo, H., Fu, W., Mattson, M.P., 1999. The endoplasmic reticulum stress-responsive protein GRP78 protects neurons against excitotoxicity and apoptosis: suppression of oxidative stress and stabilization of calcium homeostasis. Exp. Neurol. 155, 302–314.

Zhao, Q., Wang, J., Levichkin, I.V., Stasinopoulos, S., Ryan, M.T., Hoogenraad, N.J., 2002. A mitochondrial specific stress response in mammalian cells. EMBO J. 21, 4411–4419.

Zinszner, H., Kuroda, M., Wang, X., Batchvarova, N., Lightfoot, R.T., Remotti, H., Stevens, J.L., Ron, D., 1998. CHOP is implicated in programmed cell death in response to impaired function of the endoplasmic reticulum. Genes Dev. 12, 982–995.

informa
healthcare

ORIGINAL ARTICLE

Vestibular function of patients with profound deafness related to *GJB2* mutation

MISATO KASAI[1], CHIERI HAYASHI[1], TAKASHI IIZUKA[1], AYAKO INOSHITA[1], KAZUSAKU KAMIYA[1], HIROKO OKADA[1], YUKINORI NAKAJIMA[1], KIMITAKA KAGA[2] AND KATSUHISA IKEDA[1]

[1]*Department of Otorhinolaryngology, Juntendo University School of Medicine, Tokyo and* [2]*National Institute of Sensory Organs, National Tokyo Medical Center, Tokyo, Japan*

Abstract

Conclusion: GJB2 mutations are responsible not only for deafness but also for the occurrence of vestibular dysfunction. However, vestibular dysfunction tends to be unilateral and less severe in comparison with that of bilateral deafness. *Objectives:* The correlation between the cochlear and vestibular end-organs suggests that some children with congenital deafness may have vestibular impairments. On the other hand, *GJB2* gene mutations are the most common cause of nonsyndromic deafness. The vestibular function of patients with congenital deafness (CD), which is related to *GJB2* gene mutation, remains to be elucidated. The purpose of this study was to analyze the relationship between *GJB2* gene mutation and vestibular dysfunction in adults with CD. *Methods:* A total of 31 subjects, including 10 healthy volunteers and 21 patients with CD, were enrolled in the study. A hearing test and genetic analysis were performed. The vestibular evoked myogenic potentials (VEMPs) were measured and a caloric test was performed to assess the vestibular function. The percentage of vestibular dysfunction was then statistically analyzed. *Results:* The hearing level of all CD patients demonstrated a severe to profound impairment. In seven CD patients, their hearing impairment was related to *GJB2* mutation. Five of the seven patients with CD related to *GJB2* mutation demonstrated abnormalities in one or both of the two tests. The percentage of vestibular dysfunction of the patients with CD related to *GJB2* mutation was statistically higher than in patients with CD unrelated to *GJB2* mutation and in healthy controls.

Keywords: *Vestibular evoked myogenic potentials, caloric test*

Introduction

Since a correlation between the peripheral auditory and vestibular systems has been identified both anatomically and phylogenetically, a subgroup of children with congenital deafness (CD) may be associated with vestibular and balance impairments [1–3]. Interestingly, the vestibular disturbance in these children gradually disappears as they grow up, probably because of a compensatory mechanism of the central nervous system. However, there have been only a few reports that conducted a detailed analysis of the vestibular function in adults with CD.

CD has been reported in approximately one child per 1000 births [1]. In more than half of these cases,

the disease is caused by gene mutation. In particular, mutation in the *GJB2* gene, which encodes Cx26 in the gap junction, is known to be a most common cause (up to 50% of such cases) [2,3]. Gap junction channels enable the neighboring cells to exchange small signaling molecules. Immunohistochemical studies have revealed that Cx26 exists not only in the cochlea but also in the vestibular organs [4]. K$^+$ cycling involving gap junction protein Cx26 in the vestibular labyrinth, which is similar to that in the cochlea, is thought to play a fundamental role in the endolymph homeostasis and sensory transduction [5]. These findings suggest that mutations in the *GJB2* gene may thus cause vestibular dysfunction.

RIGHTSLINK()

In this study, the relationship between *GJB2* gene mutation and vestibular dysfunction in adults with CD was investigated to confirm whether or not there are any abnormalities associated with the vestibular function.

Material and methods

Subjects

The subjects in this prospective study included 21 patients with CD and 10 healthy volunteers. The patients were excluded from the study if they were being treated with ototoxic drugs or if they had a cytomegalovirus infection, bacterial meningitis, external and middle ear pathological findings, or other risk factors for inner ear damage. No participants had syndromic deafness due to pigmentary retinopathy, nephropathy, goiter, or any other diseases. Patients with vestibular dysfunction due to head trauma, brain tumor, Meniere's disease, or other conditions were also excluded from the study. All subjects underwent an otoscopic examination and were found to have a normal tympanic membrane. Audiometric testing was performed in a double-walled, sound-treated booth. All patients gave their informed consent in writing and the study was approved by the Ethics Committee of Juntendo University School of Medicine.

Genetic analysis

DNA was extracted from peripheral blood leukocytes of the subjects. The coding region of *GJB2* was amplified by PCR using the primers *GJB2*-2F 5'-GTGTGCATTCGTCTTTTCCAG-3' and *GJB2*-2R 5'-GCGACTGAGCCTTGACA-3'. The PCR products were sequenced using the PCR primers and sequence primers *GJB2*-A 5'-CCACGC-CAGCGCTCCTAGTG-3' and *GJB2*-B 5'-GAA-GATGCTGCTGCTTGTGTAGG-3'. These were visualized using an ABI Prism 310 Analyzer (PE Applied Biosystems, Tokyo, Japan).

Vestibular evoked myogenic potentials

The vestibular evoked myogenic potentials (VEMPs) were measured as described in a previous report [6]. Both sound stimuli of clicks (0.1 ms, 95 dBnHL) and short tone burst (500 Hz; rise/fall time, 1 ms, 95 dBnHL) were presented to each side of the ear through the headphones using a Neuropack evoked-potential recorder (Nihon Kohden Co. Ltd,

Tokyo, Japan). The surface electromyographic activity was recorded with the patient in the supine position from symmetrical sites over the upper half of each sternocleidomastoid (SCM) muscle with a reference electrode on the lateral end of the upper sternum. During recording, the subjects were instructed to lift their head up or to turn the contralateral side to induce hypertonicity of the SCM. Thereafter, the electromyographic signals from the stimulated side of the SCM muscle were amplified.

Caloric test

The caloric test in the current study was performed as described elsewhere [7]. Briefly, 2 ml of ice-water (at 4°C) was irrigated in the external auditory meatus to induce a thermal gradient across the horizontal semicircular canal of one ear. The duration of horizontal and vertical nystagmus was recorded. The results were compared between the right and left ears.

Statistical analysis

The data are expressed as the mean ± SD. Statistical analyses were conducted using a non-repeated measures analysis of variance (ANOVA). Significant effects were further analyzed by post hoc multiple comparison tests using the Student-Newman-Keuls test. A value of $p < 0.05$ was considered to indicate statistical significance.

Results

Hearing test

The pure-tone averages of 0.5, 1.0, and 2.0 kHz are shown in Table I. The hearing impairments of CD patients ranged from severe (71–95 dB) to profound (>95 dB). The hearing levels of all controls were at the normal level (<30 dB; data not shown).

Genetic analysis

GJB2 mutations were found in nine CD patients (Table I). All three mutations have been described previously in association with deafness. Among these mutations, 235delC mutation was found in eight patients. One nonsense mutation (Y136X) and one frameshift mutation (176-191del) were also identified. In six patients with a homozygous *GJB2* mutation and one patient with a compound heterozygous

Table I. Results of hearing level, genetic analysis, and vestibular function of subjects with congenital deafness (CD)

Case no.	Hearing level (dB)		Sex	Age (years)	Mutation in *GJB2*	VEMPs	Caloric test
	Left	Right					
Patients with *GJB2*-related CD							
1	86	98	M	26	Homo 235delC	Right decreased	Left CP
2	106	108	M	25	Homo 235delC	Right decreased	Normal
3	108	106	M	28	Homo 235delC	Right decreased	Normal
4	108	106	M	37	Homo 235delC	Normal	Right CP
5	100	106	M	32	Homo 235delC	Normal	Right poor/left CP
6	80	91	M	25	Homo 235delC	Normal	Normal
7	115	108	M	25	Y136X/235delC	Normal	Normal
Patients without *GJB2*-related CD							
8	98	98	F	24		Left decreased	Bilateral CP
9	98	115	M	26		Normal	Bilateral CP
10	97	97	M	20		Normal	Normal
11	111	108	M	31		Normal	Normal
12	100	104	F	34		Normal	Normal
13	98	95	M	21		Normal	Normal
14	91	91	M	24		Normal	Normal
15	99	101	F	26		Normal	Normal
16	99	95	F	23		Normal	Normal
17	80	68	M	27		Normal	Normal
18	96	95	M	27		Normal	Normal
19	85	73	M	23		Normal	Normal
Patients with heterozygous *GJB2* mutation							
20	73	100	M	25	Hetero 235delC	Normal	Normal
21	97	98	M	25	Hetero 176-191del16	Normal	Normal

CP, canal paresis; Poor, nystagmus was obviously weak.

mutation (case nos 1–7); their profound deafness was thought to be caused by a *GJB2* mutation. No *GJB2* mutation was identified in any of the controls.

Vestibular function

No patients or controls had any subjective symptoms of vertigo. Table I shows the results of the vestibular function in all CD patients. Abnormal responses of VEMPs and the caloric test in CD with a *GJB2*-related mutation were observed in three patients each (case nos 1–5). Three patients with a homozygous *GJB2* mutation showed asymmetrical responses in VEMPs (case nos 1–3). Three patients with a homozygous *GJB2* mutation showed asymmetrical responses in the caloric test (case nos 1, 4, and 5). One of them showed both VEMPs and the caloric test

asymmetrical responses (case no. 1). One patient with a homozygous *GJB2* mutation and one patient with compound heterozygous *GJB2* mutation showed normal responses in both VEMPs and the caloric test (case nos 6 and 7). It is notable that five of the six patients with a homozygous 235delC mutation showed no abnormalities in either test. Two heterozygous patients (case nos 20 and 21) showed normal responses in both tests.

Two CD patients with no *GJB2* mutation exhibited abnormal findings for the vestibular tests (case nos. 8 and 9). One patient showed a unilateral reduction in VEMPs and bilateral canal paresis (case no. 8). Bilateral canal paresis was also observed in another patient (case no. 9).

All the controls with normal hearing showed normal responses in both the VEMPs and the caloric test (data not shown).
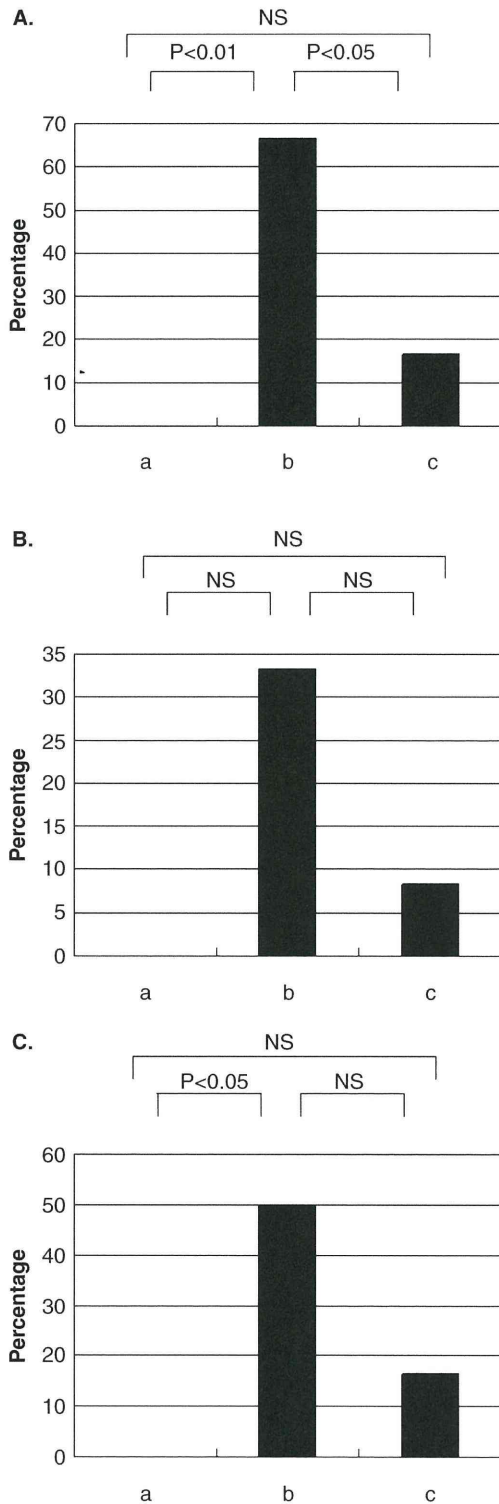
Figure 1. Comparison of the incidence of abnormality in the vestibular tests among the three groups. (A) Percentage showing abnormality in VEMPS and/or caloric test. (B) Percentage showing abnormality in VEMPs. (C) Percentage showing abnormality in the caloric test. a, Controls; b, *GJB2*-related CD subjects; c, CD subjects without *GJB2* mutations.

Statistical analysis of vestibular function in the three groups

Figure 1 shows a comparison of the controls, patients with CD related to a *GJB2* mutation, and those with CD without a *GJB2* mutation. The CD patients with *GJB2* heterozygous mutation were excluded from this statistical analysis, since their symptoms of hearing impairment are not necessarily caused by the *GJB2* mutation alone. Vestibular dysfunction showing an abnormality in VEMP and/or the caloric test significantly increased in patients with *GJB2*-related CD in comparison with those with CD without *GJB2* mutation ($p < 0.05$) and the controls ($p < 0.01$), whereas no difference was observed between CD without a *GJB2* mutation and the controls (Fig. 1A). No differences in the incidence of abnormality in VEMPs were observed among the three groups (Fig. 1B). The incidence of abnormalities in the caloric test in patients with *GJB2*-related CD differed significantly from that in the controls, but the other two comparisons were not significant (Fig. 1C).

Discussion

In this study, vestibular tests were performed in CD patients with or without a *GJB2* mutation by measuring the VEMPs and using the caloric test. Only one report has previously investigated the vestibular function of patients with *GJB2*-related CD [8]. The authors noted that five of the seven patients showed no VEMP responses bilaterally and that only one case had a unilateral pathological response in the caloric test, which led to the conclusion that CD with a *GJB2* mutation is associated with severe saccular dysfunction. However, in the present study, there were no patients showing the absence of both VEMP and a caloric response. Todt et al. [8] showed the existence of *GJB2* mutations that do not cause CD (polymorphisms), thus suggesting a considerable bias. Furthermore, patients with low-grade hearing loss were included in their study. In contrast, all of the *GJB2* mutations detected in the present study are known to cause CD in the Asian population [9]. In addition, the present study included only patients with severe to profound hearing loss, which would therefore clarify the correlation between CD and *GJB2* mutations. Among the seven patients with *GJB2*-related CD, five (71.4%) showed abnormal responses in either or both tests. The incidence was apparently and significantly higher than that in patients with CD without a *GJB2* mutation (2/13: 15.4%). Moreover, the incidence in the controls significantly differed from that in patients with CD related to a *GJB2*

mutation but not in those with CD without *GJB2* mutation. Therefore, these findings support the hypothesis that *GJB2* mutations play a critical role in the disturbance of the vestibular function.

GJB2 mutations cause profound deafness and the associated mechanism has been discussed in several studies [10,11]. A recent study showed that *GJB2* is indispensable in the normal development of the organ of Corti and normal hearing on the basis of the study in *Gjb2* dominant-negative mutant mice [12]. Despite the widespread expression of Cx26 in both the cochlear and vestibular organs [4], the vestibular function impairment of the patients with a *GJB2* mutation is not as severe as the hearing dysfunction observed in the present study. Two hypotheses have been proposed to explain this inconsistency between hearing and balance function. One hypothesis is based on the fact that two temporal bone studies performed in patients with *GJB2*-related hearing impairment in the previous study revealed that one patient had mild vestibular hydrops and saccular degeneration, while another patient had a dysplastic neuroepithelium of the saccule [13,14]. This suggests that a *GJB2* mutation can cause morphological dysplasia in not an entire organ, but in part of the vestibular organs. This is contrast to the cochlea of these patients, which showed nearly total dysplasia of the organ of Corti. These histopathological studies support the results of the vestibular dysfunction of patients with *GJB2*-related CD in the present study. The other hypothesis is based on the presence of several connexins such as Cx26, Cx30 (encoded by *GJB6*), Cx31 (encoded by *GJB3*), and Cx32 (encoded by *GJB1*) in the inner ear. A previous study showed all of these connexins to be distributed in the vestibular organs [15]. Cx30 gene knockout mice had hair cell loss in the saccule, which was restored by the over-expression of the Cx26 gene [16]. Therefore, the specific loss of Cx30 causes vestibular dysfunction, which can be compensated by other types of connexins. The present clinical study in which a complete defect of Cx26 resulted in a definitive but partial dysfunction of vestibular end organs can be explained by the compensation of other connexins normally expressed in the vestibule. Further studies are required to clarify the relationship between connexins and the vestibular function.

Although there was a statistically significant difference in the objective examination of the vestibular function among patients with *GJB2*-related CD, those with CD without a *GJB2* mutation, and healthy controls, none of these subjects had any vestibular symptoms regardless of the presence or absence of a *GJB2* mutation. The peripheral

vestibular dysfunction predicted in individuals with the *GJB2* mutation may be compensated by the central vestibular system in young patients with deafness, as shown in the present study. However, aging is known to affect both the peripheral and central vestibular system [17]. In patients with a *GJB2* mutation, the vestibular symptoms may progress with aging. Another problematic point regarding patients with CD related to *GJB2* mutations is cochlear implantation, which has been reported to cause vestibular dysfunction, such as a reduction of the caloric responses [18] and a decrease in the VEMP responses [19]. It is thought that the mechanical damage caused by the insertion of the electrode may induce vestibular dysfunction [20]. In the present study, four patients with *GJB2*-related deafness showed unilateral vestibular dysfunction, while only one of them had bilateral dysfunction. Therefore, it should be emphasized that the assessment of the vestibular function in patients with *GJB2*-related CD is important to determine which side of the ear should be selected to insert the cochlear implant.

Conclusions

A *GJB2* mutation is responsible not only for deafness but also for vestibular dysfunction. However, such vestibular dysfunction is likely to be unilateral and less severe in patients with a *GJB2* mutation than in those with bilateral deafness.

Declaration of interest: The authors report no conflicts of interest. The authors alone are responsible for the content and writing of the paper.

References

[1] Morton NE. Genetic epidemiology of hearing impairment. Ann N Y Acad Sci 1991;630:16–31.
[2] Denoyelle F, Marlin S, Weil D, Moatti L, Chauvin P, Garabedian EN, et al. Clinical features of the prevalent form of childhood deafness, DFNB1, due to a connexin-26 gene defect: implications for genetic counselling. Lancet 1999;353:1298–303.
[3] Murgia A, Orzan E, Polli R, Martella M, Vinanzi C, Leonardi E, et al. Cx26 deafness: mutation analysis and clinical variability. J Med Genet 1999;36:829–32.
[4] Masuda M, Usami S, Yamazaki K, Takumi Y, Shinkawa H, Kurashima K, et al. Connexin 26 distribution in gap junctions between melanocytes in the human vestibular dark cell area. Anat Rec 2001;262:137–46.
[5] Wangemann P. K(+) cycling and its regulation in the cochlea and the vestibular labyrinth. Audiol Neurootol 2002;7:199–205.
[6] Jin Y, Nakamura M, Shinjo Y, Kaga K. Vestibular-evoked myogenic potentials in cochlear implant children. Acta Otolaryngol 2006;126:164–9.

[7] Yukiko S, Yulian J, Kimitaka K. Assessment of vestibular function of infants and children with congenital and acquired deafness using the ice-water caloric test, rotational chair test and vestibular-evoked myogenic potential recording. Acta Otolaryngol 2007;127:736–47.

[8] Todt I, Hennies HC, Basta D, Ernst A. Vestibular dysfunction of patients with mutations of Connexin 26. Neuroreport 2005;16:1179–81.

[9] Ohtsuka A, Yuge I, Kimura S, Namba A, Abe S, Van Later L, V, et al. GJB2 deafness gene shows a specific spectrum of mutations in Japan, including a frequent founder mutation. Hum Genet 2003;112:329–33.

[10] Kudo T, Kure S, Ikeda K, Xia AP, Katori Y, Suzuki M, et al. Transgenic expression of a dominant-negative connexin26 causes degeneration of the organ of Corti and non-syndromic deafness. Hum Mol Genet 2003;12:995–1004.

[11] Cohen-Salmon M, Ott T, Michel V, Hardelin JP, Perfettini I, Eybalin M, et al. Targeted ablation of connexin26 in the inner ear epithelial gap junction network causes hearing impairment and cell death. Curr Biol 2002;12: 1106–11.

[12] Inoshita A, Iizuka T, Okamura HO, Minekawa A, Kojima K, Furukawa M, et al. Postnatal development of the organ of Corti in dominant-negative Gjb2 transgenic mice. Neuroscience 2008;156:1039–47.

[13] Griffith AJ, Yang Y, Pryor SP, Park HJ, Jabs EW, Nadol JB Jr, et al. Cochleosaccular dysplasia associated with a connexin 26 mutation in keratitis-ichthyosis-deafness syndrome. Laryngoscope 2006;116:1404–8.

[14] Jun AI, McGuirt WT, Hinojosa R, Green GE, Fischel-Ghodsian N, Smith RJ. Temporal bone histopathology in connexin 26-related hearing loss. Laryngoscope 2000;110:269–75.

[15] Forge A, Becker D, Casalotti S, Edwards J, Marziano N, Nevill G. Gap junctions in the inner ear: comparison of distribution patterns in different vertebrates and assessment of connexin composition in mammals. J Comp Neurol 2003;467:207–31.

[16] Qu Y, Tang W, Dahlke I, Ding D, Salvi R, Sohl G, et al. Analysis of connexin subunits required for the survival of vestibular hair cells. J Comp Neurol 2007;504: 499–507.

[17] Gazzola JM, Perracini MR, Gananca MM, Gananca FF. Functional balance associated factors in the elderly with chronic vestibular disorder. Braz J Otorhinolaryngol 2006;72:683–90.

[18] Buchman CA, Joy J, Hodges A, Telischi FF, Balkany TJ. Vestibular effects of cochlear implantation. Laryngoscope 2004;114:1–22.

[19] Ernst A, Todt I, Seidl RO, Eisenschenk A, Blodow A, Basta D. The application of vestibular-evoked myogenic potentials in otoneurosurgery. Otolaryngol Head Neck Surg 2006;135:286–90.

[20] Jin Y, Shinjo Y, Akamatsu Y, Ogata E, Nakamura M, Kianoush S, et al. Vestibular evoked myogenic potentials evoked by multichannel cochlear implant – influence of C levels. Acta Otolaryngol 2008;128:284–90.

実験動物を用いた内耳細胞治療研究へのアプローチ

神谷　和作・池田　勝久

Experimental Approaches to Inner Ear Cell Therapy Using Laboratory Animals

Kazusaku Kamiya and Katsuhisa Ikeda

(Juntendo University School of Medicine)

Recently, a number of clinical studies on cell therapy have been reported and used in clinical practice for several intractable diseases. Inner ear cell therapy for sensorineural hearing loss also has been studied using some laboratory animals, although to date reports on successful hearing recovery have been few.

Previously, we developed a novel rat model of acute sensorineural hearing loss due to fibrocyte dysfunction induced by a mitochondrial toxin and performed cell therapy with bone marrow mesenchymal stem cells (MSCs). In this study, we injected MSCs into the lateral semicircular canal; a number of these stem cells were then detected in the injured area in the lateral wall. Rats with transplanted MSCs in the lateral wall demonstrated a significantly higher hearing recovery ratio than the untreated controls. These results suggested that mesenchymal stem cell transplantation into the inner ear may be a promising therapy for patients with sensorineural hearing loss due to degeneration of cochlear fibrocytes.

In this article, we review studies on inner ear cell therapy using some laboratory animals including rodents such as mice and rats, and primates such as cynomologus monkeys (Macaca fascicularis).

Key words : inner ear, cell therapy, sensoryneural hearing loss, stem cell

はじめに

感音性難聴の原因は多岐にわたるが，近年の遺伝子改変動物開発技術の向上や多種のモデル動物の開発により多くの病態メカニズムが解明に近づいている．すべての先天性疾患の中でも頻度の高い遺伝性難聴においては，難聴家系や突然変異難聴マウスの遺伝子解析によって多くの遺伝性難聴原因遺伝子が同定されている．初期に発見された遺伝性難聴の原因の多くは内耳有毛細胞の変性または機能的・形態的異常であったため，多くの研究者が有毛細胞を中心に難聴の病態メカニズム解明に取り組んできた．哺乳類の有毛細胞は再生能力を持たないため遺伝子導入などによる有毛細胞再生の誘導も盛んに研究されてきた[1][2]．その一方で内耳への細胞移植による有毛細胞の修復の試みも行われているが，特殊なリンパ液で満たされた内耳の構造的特徴から，聴力を保持しつつ標的部位に移植細胞を到達させ分化させることは容易では

ない．そのため有毛細胞の修復には多種のモデル動物を用いた多くの検討実験が必要と考えられる．近年有毛細胞以外にも蝸牛線維細胞などの機能異常が単独で難聴病態の引き金となることも明らかとなっており，多様な治療戦略が求められている．幹細胞の損傷部への移動能力や組織環境（ニッシェ，niche）による分化誘導を十分に検討すれば細胞治療は内耳組織変性に対する治療にも応用可能と考えられる．著者らの報告では実験的に蝸牛線維細胞のみに傷害を与えたラットへ半規管外リンパ液を経由した細胞液還流法を用いることにより，損傷部の修復と聴力回復率を高めることに成功した[3]．現在はヒト疾患に近い遺伝性難聴モデル動物への各種の幹細胞移植に取り組んでいる．また，サル類を用いた細胞移植アプローチの検討も今後応用性を高めるためには非常に重要であるため現在,カニクイザルによる検討を行っている．各種のモデル動物の特徴を考慮した細胞移植実験検討を

順天堂大学耳鼻咽喉科学教室

積み重ねることにより，将来的には有毛細胞も標的とした多様な難聴に対する聴力回復も不可能ではないと考えられる．本稿では各種実験動物を用いた内耳への細胞治療研究に関する知見について報告する．

内耳細胞治療実験に用いられる実験動物

　外傷，騒音，感染，薬物障害，血流障害，加齢に起因する聴覚障害動物モデルは多く開発されており，細胞治療研究のための有用な実験モデルとして活用することができる．著者らはミトコンドリア阻害薬を用いて蝸牛線維細胞のみに損傷を与えるモデルラットを開発し，この細胞移植実験に成功している．しかしこのような実験的に内耳損傷を誘導した動物モデルがヒトと同等な内耳組織障害および機能的障害を忠実に再現しているかという点に関しては実証することは困難である．これに対し原因タンパク質がすでに特定されている遺伝子改変動物または突然変異動物はヒト遺伝性難聴の病態の多くが一致していると考えられる．細胞移植によりそのタンパク質が担う機能を回復させることができれば，幹細胞が正常に分化し失われていたタンパク質機能を取り戻した結果として聴力が回復したことを実証しやすい．有毛細胞の変性が顕著にみられるモデル動物としては，アッシャー症候群原因遺伝子（Pcdh15[4]，Cdh23[5]，Sans[6]，Harmonin[7]，MyosinVIIa[8]など）の突然変異動物あるいは遺伝子改変動物が，明白な表現型を持つため有毛細胞の研究に広く用いられている．これらの進行性の組織変性は重度であり有毛細胞の変性から連鎖的にラセン神経節細胞の消失へとつながる場合も多い．そのため細胞治療による細胞の生着・分化の検討は可能であるが聴力改善の検討は現段階で容易ではないと思われる．蝸牛線維細胞を標的とした場合，有毛細胞変性を伴わず蝸牛線維細胞のみに変性を持つ Brn4 欠損マウス[9]，Otospiralin 欠損マウス[10] が有効であると考えられる．これらの聴力改善の可能性は有毛細胞を標的とした細胞治療より格段に高いと思われる．ヒト遺伝性難聴でもっとも高頻度に出現するコネキシン26の遺伝子欠損マウスおよび優性阻害トランスジェニックマウス[11]は同遺伝子が蝸牛線維細胞および支持細胞に主に発現するため，著者らの行った骨髄間葉系幹細胞移植も有効であると考えられる．

蝸牛線維細胞を標的とした骨髄間葉系幹細胞移植

　蝸牛ラセン靭帯およびラセン板縁を構成する蝸牛線維

細胞はナトリウムポンプとギャップジャンクションによる蝸牛内イオンの能動輸送および受動輸送という単純な機能を担っている．しかしながら蝸牛線維細胞の傷害は複数の先天性および後天性難聴の主要因となることが示され，その重要性が近年示唆されている．とくにヒト非症候性難聴 DFN3 の原因因子 Brn4 の遺伝子欠損マウス[9] や otospiralin 欠損マウス[10] では蝸牛線維細胞の変性を主要因とした聴力低下が実証され，有毛細胞を含むコルチ器と同様に正常聴力を維持するうえで重要性の高い細胞群であることが明確に示された．また複数の加齢性難聴モデル動物においても蝸牛線維細胞の変性が他の細胞に先立ち開始することが報告されている[12]〜[14]．また蝸牛線維細胞は単一細胞としての機能が単純であるにもかかわらず内耳機能における重要性が高いという点から，高度に分化した有毛細胞に比べて細胞治療が成功する可能性が格段に高いと考えられる．これらのことから蝸牛線維細胞は多種の感音難聴に対する新規治療法確立への重要な標的となりうると考えられる．著者らは薬剤
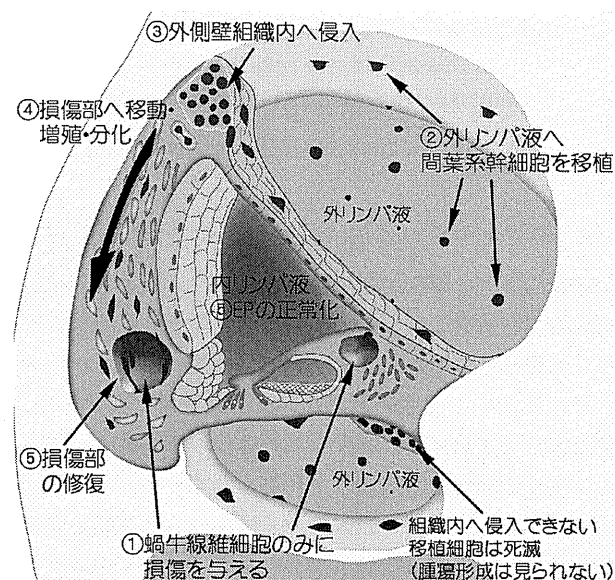

図 1　蝸牛線維細胞をターゲットとした骨髄間葉系幹細胞移植での損傷部の修復および推測された移植細胞の移動経路
薬剤投与によりらせん靭帯およびらせん板縁に選択的に損傷を与え①，その後外リンパ液へ骨髄から採取した間葉系幹細胞を半規管からの還流により投与②した結果，投与した間葉系幹細胞が外側壁組織内へ進入し④，移動・増殖・分化④により損傷部の修復⑤を促進し高周波数音域の聴力回復率が有意に上昇した．（Reprinted from Am J Pathol Am J Pathol 2007, 171：214 〜 226 with permission from the American Society For Investigative Pathology）

局所投与により蝸牛線維細胞の二点にのみ限局的なアポトーシスを起こすモデルラットを開発し[15][16]，半規管からの骨髄間葉系幹細胞の外リンパ液還流投与を行った．その結果，移植 11 日後の高音域（40 KHz）の聴力回復が有意に促進し，外側壁の蝸牛線維細胞損傷部に多数の移植細胞が観察された．組織内には腫瘍化を示す移植細胞は観察されなかった．移植細胞は蝸牛外側壁の頂回転側，外リンパ液に面している部分で多くみられ，この部位を中心に蝸牛組織に侵入し損傷部まで移動したと考えられる．損傷部ではコネキシンの発現とともに隣接細胞と接合する移植細胞が観察され，イオン輸送経路の回復による内リンパ液 K^+ 濃度の正常化が聴力回復に寄与したと推測される（図1）[3]．

内耳への細胞投与法

著者らの初期の移植検討実験では，ラット蝸牛管付近より細胞液投与を試みた際はどの部位でも手術による永続的な聴力低下がみられ，蝸牛組織には繊維化が認められた．著者らは Iguchi らの方法[17]を参考にラットの後半規管および外側半規管にそれぞれ小孔を開け，片側から微小チューブを挿入し細胞液（1×10^5cells/20 μl）での 10 分間の還流を行った．この方法では手術による聴力低下はほとんどみられず，大量の細胞を蝸牛内に導入することができるため内耳細胞治療に適した投与法であると思われる．また新生児難聴スクリーニング直後の早期治療を想定した内耳への投与方法として，Iizuka ら[18]は生後 0 日齢の幼若マウスへ微小ガラス管を用いて遺伝子治療用ウイルス液を非侵襲的に外リンパ液内へ注入することに成功している．同方法は非侵襲性を必要とする幼若個体への細胞注入にも応用可能であると考えられる．この方法では外リンパ液の漏出がほとんどないため，少量であれば非侵襲的に細胞液を注入することができる．細胞移植用としてはガラス管先端の直径をパッチクランプ用のプラーで微調整することで利用可能と考えられる．

サル類を用いた細胞治療研究の重要性

げっ歯類を用いることにより，新規な細胞治療法の開発や多くの分子生物学的，生理学的データの取得が期待できる．一方でげっ歯類ではその生理・代謝機能が必ずしもヒトを忠実に反映していない部分もあり，ヒトへの外挿面で必ずしも一致した効果を得られない可能性も考えられる．たとえばヒトと同様サル類でも出生直後に外部の音刺激を入力することができると考えられるが，マウスやラットでは生後約10日齢までは内耳が未成熟であるため音の入力が開始しない．新生児難聴スクリーニング直後の細胞治療を目的とした検討の場合などはとくに成熟レベルによる細胞治療の有効性や安全性が大きく異なることが予想されるため，実験用サルによる安全性・
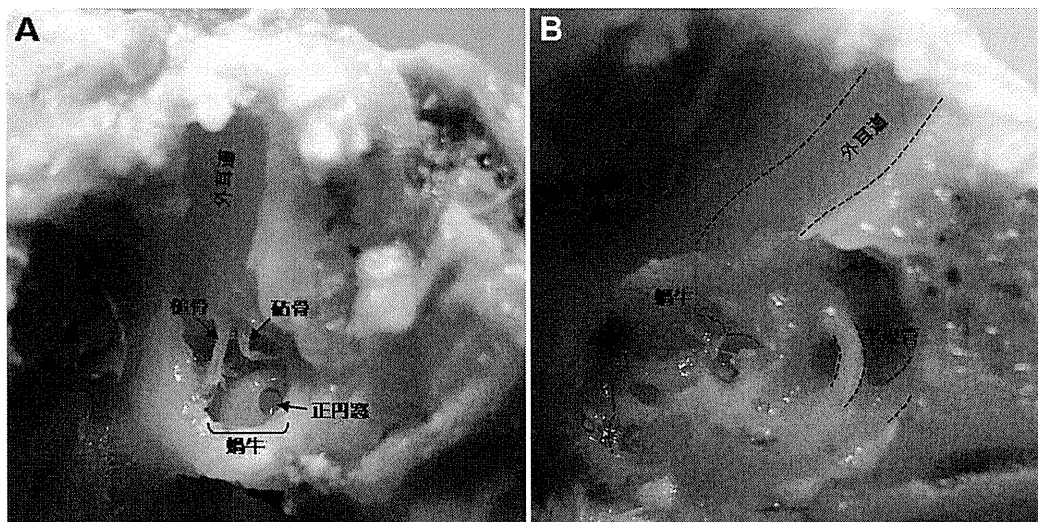

図2　成熟カニクイザルの内耳
　　A．上顎側より削開し外耳道，耳小骨，蝸牛を露出した．
　　B．さらに内耳周囲を削開し蝸牛内部および半規管を露出した．ヒトとほぼ同様の内耳構造およびその周囲構造がみられる．

有効性の評価が将来的に非常に重要になると考えられ
る．マウスやラットで開発された細胞治療法を臨床応用
へ近づけるためには，サル類（カニクイザル等）を用い，
それらの安全性評価データをヒトへ外挿する必要があ
る．サル類を用いた細胞治療実験では，マウスやラット
による基礎データをもとに有効かつ安全な移植方法や移
植細胞の種類，成熟ステージを評価することが重要であ
ると考えられる．現在，カニクイザル頭部を用いた細胞
治療アプローチに関する検討実験を行っている（図 2）．
カニクイザル側頭骨は手術の際に削開を進める角度など
がヒトと多少異なるが，内耳構造やその周囲構造に共通
点が多く細胞移植手術による半規管や正円窓へのアプ
ローチもヒトのモデルとして非常に有効であると考えら
れる．

各種実験動物の特徴

　マウスに関していえば，近年膨大な種類の遺伝子改変
マウスが各国でされ，データベース化や共有研究資材と
して分配されているものもある．病態変化や細胞移植後
の変化を分子生物学的手法により解析する場合は情報や
各種実験ツールの多さからマウスが他の実験動物と比較
し圧倒的に有用性・汎用性が高いと考えられる．各種幹
細胞の入手もマウスでは比較的容易である．しかし内耳
への細胞の局所投与を必要とする場合はアプローチの方
法やターゲットとする疾患に対し最適な病態モデルを得
るため，マウス以外のげっ歯類（モルモット，スナネズ
ミ，ラット）も十分有効に活用できる．半規管経由の細
胞移植に関していえば，げっ歯類では外側半規管および
後半規管が側頭骨表面に露出しているためアプローチが
容易である．

　サル類に関していえば，研究コスト面での負担が大き
いが臨床応用へ向けての安全性・有効性評価の面で必須
の実験動物といえる．カニクイザル（*Macaca fascicularis*）
は我が国でも保有する施設が多数存在し，多くの動物実
験に利用されている．前述したように内耳周辺の組織構
造，生理機能がヒトとほぼ同等と考えられるため，げっ
歯類で有効性が実証された細胞治療法をカニクイザルに
おいて有効性および安全性を再評価することが臨床応用
に向けて重要であると考えられる．

参考文献

1) Izumikawa M, Minoda R, Kawamoto K, et al. : Auditory hair cell replacement and hearing improvement by Atoh1 gene therapy in deaf mammals. Nat Med **11**: 271-276, 2005.

2) Gubbels SP, Woessner DW, Mitchell JC, et al. : Functional auditory hair cells produced in the mammalian cochlea by in utero gene transfer. Nature **455**: 537-541, 2008.

3) Kamiya K, Fujinami Y, Hoya N, et al. : Mesenchymal stem cell transplantation accelerates hearing recovery through the repair of injured cochlear fibrocytes. Am J Pathol **171**: 214-226, 2007.

4) Alagramam KN, Murcia CL, Kwon HY, et al. : The mouse Ames waltzer hearing-loss mutant is caused by mutation of Pcdh15, a novel protocadherin gene. Nat Genet **27**: 99-102, 2001.

5) Di Palma F, Holme RH, Bryda EC, et al. : Mutations in Cdh23, encoding a new type of cadherin, cause stereocilia disorganization in waltzer, the mouse model for Usher syndrome type 1D. Nat Genet **27**: 103-107, 2001.

6) Kikkawa Y, Shitara H, Wakana S, et al. : Mutations in a new scaffold protein Sans cause deafness in Jackson shaker mice. Hum Mol Genet **12**: 453-461, 2003.

7) Johnson KR, Gagnon LH, Webb LS, et al. : Mouse models of USH1C and DFNB18: phenotypic and molecular analyses of two new spontaneous mutations of the Ush1c gene. Hum Mol Genet **12**: 3075-3086, 2003.

8) Gibson F, Walsh J, Mburu P, et al. : A type VII myosin encoded by the mouse deafness gene shaker-1. Nature **374**: 62-64, 1995.

9) Minowa O, Ikeda K, Sugitani Y, et al. : Altered cochlear fibrocytes in a mouse model of DFN3 nonsyndromic deafness. Science **285**: 1408-1411, 1999.

10) Delprat B, Ruel J, Guitton MJ, et al. : Deafness and cochlear fibrocyte alterations in mice deficient for the inner ear protein otospiralin. Mol Cell Biol **25**: 847-853, 2005.

11) Kudo T, Kure S, Ikeda K, et al. : Transgenic expression of a dominant-negative connexin26 causes degeneration of the organ of Corti and non-syndromic deafness. Hum Mol Genet **12**: 995-1004, 2003.

12) Hequembourg S and Liberman MC : Spiral ligament pathology: a major aspect of age-related cochlear degeneration in C57BL/6 mice. J Assoc Res Otolaryngol **2**: 118-129, 2001.

13) Spicer SS and Schulte BA : Spiral ligament pathology in quiet-aged gerbils. Hear Res **172**: 172-185, 2002.

14) Wu T and Marcus DC : Age-related changes in cochlear endolymphatic potassium and potential in CD-1 and CBA/CaJ mice. J Assoc Res Otolaryngol **4**: 353-362, 2003.

15) Hoya N, Okamoto Y, Kamiya K, et al. : A novel animal model of acute cochlear mitochondrial dysfunction. Neuroreport **15**: 1597-1600, 2004.

16）Okamoto Y, Hoya N, Kamiya K, et al. : Permanent threshold shift caused by acute cochlear mitochondrial dysfunction is primarily mediated by degeneration of the lateral wall of the cochlea. Audiol Neurootol **10**：220-233, 2005.

17）Iguchi F, Nakagawa T, Tateya I, et al. : Surgical techniques for cell transplantation into the mouse cochlea. Acta Otolaryngol Suppl **551**：43-47, 2004.

18）Iizuka T, Kanzaki S, Mochizuki H, et al. : Noninvasive in vivo delivery of transgene via adeno-associated virus into supporting cells of the neonatal mouse cochlea. Hum Gene Ther **19**：384-390, 2008.

別刷請求先：神谷和作
〒171-0021　東京都文京区本郷 2 -1-1
順天堂大学医学部耳鼻咽喉科学教室

難聴に対する内耳細胞治療法の開発

Inner ear cell therapy for sensorineural hearing loss

神谷和作
Kazusaku KAMIYA
順天堂大学医学部耳鼻咽喉科学教室

◎内耳は特殊なリンパ液で満たされた独特な構造をもち，血液−内耳関門とよばれる血管系を有するため，内耳有毛細胞やその周辺細胞への薬物的アプローチが難しい．しかし，移動能・多分化能を兼ね備えた幹細胞による内耳細胞治療の方法が確立すれば，難聴の根本的治療への有効なツールになると考えられる．近年の内耳再生医療に関する基礎研究分野は，*in vitro* での有毛細胞への分化誘導において年々進歩している．最近では培養シャーレ内で鳥類細胞から聴毛を有する有毛細胞への分化誘導も可能となっており[1]，細胞工学的分野では一定の成果が得られている．しかし，それらの細胞を移植により内耳組織へ生着させ，同時に機能的補足や組織修復によって聴力回復を誘導する細胞治療の試みは成功例が少なく，引用度の高い論文での報告も少ない．聴力回復を目的とした内耳細胞治療法を開発するためには移植細胞の生着と機能発現を同時に考慮し，内耳の解剖学的特徴および各細胞の生理学的特徴を十分に理解することが重要であると考えられる．著者らの報告では，実験的に蝸牛線維細胞のみに傷害を与えたラットへ半規管外リンパ液を経由した細胞液灌流法を用いることにより，損傷部の修復と聴力回復率を高めることに成功した[2]．現在は，ヒト疾患に近い遺伝性難聴モデル動物への各種の幹細胞移植に取り組んでいる．蝸牛線維細胞のような，修復が困難ではないが聴力維持に不可欠な細胞を標的に検討を積み重ねることにより，将来的には有毛細胞も標的とした多様な難聴に対する聴力回復も不可能ではないと考えられる．本稿では，とくに各種幹細胞や遺伝子改変動物を用いた内耳への細胞治療に関する知見について報告する．

Key word ：内耳，蝸牛，有毛細胞，蝸牛線維細胞，骨髄間葉系幹細胞

背景

難聴の原因は多岐にわたるが，近年の遺伝子改変動物開発技術の向上や多種のモデル動物の開発により，多くの病態メカニズムが解明に近づいている．すべての先天性疾患のなかでも頻度の高い遺伝性難聴においては，難聴家系や突然変異難聴マウスの遺伝子解析によって多くの遺伝性難聴原因遺伝子が同定されている．初期に発見された遺伝性難聴の原因の多くは内耳有毛細胞の変性または機能的・形態的異常であったため，多くの研究者が有毛細胞を中心に難聴の病態メカニズム解明に取り組んできた．哺乳類の有毛細胞は再生能力をもたないため遺伝子導入などによる有毛細胞再生の誘導も盛んに研究されてきた[3,4]．その一方で，内耳への細胞移植による有毛細胞の修復の試みも行われているが，特殊なリンパ液で満たされた内耳の構造的特徴から，聴力を保持しつつ標的部位に移植細胞を到達させ分化させることは容易ではない．そのため有毛細胞の修復にはモデル動物を用いた多くの検討実験が必要と考えられる．近年，有毛細胞以外にも蝸牛線維細胞などの機能異常が単独で難聴病態の引き金となることも明らかとなっており，多様な治療戦略が求められている．

幹細胞の損傷部への移動能力や組織環境(ニッシェ，niche)による分化誘導を十分に検討すれば，細胞治療は未だ根本的治療法の存在しない内耳組織変性に対する治療にきわめて有効であると考えられる．